THE ASTROPHYSICAL JOURNAL, **266**:596–601, 1983 March 15

VLA OBSERVATIONS OF WARM NH_3 ASSOCIATED WITH MASS OUTFLOWS IN W51

PAUL T. P. HO
Radio Astronomy Laboratory, University of California, Berkeley
AND
REINHARD GENZEL[1] AND ANIRUDDHA DAS
Department of Physics, University of California, Berkeley
Received 1982 July 19; accepted 1982 September 9

ABSTRACT

We present VLA observations of the $(J, K) = (3,3)$ inversion line of NH_3 toward the distant H II region complex in W51. Three small (~ 0.1 pc), warm (~ 100 K) NH_3 condensations are found coincident with every one of the H_2O and OH maser sources in the region. This positional coincidence, as well as the observed large line widths (≥ 10 km s^{-1}), suggests that the localized NH_3 emission arises from dense molecular condensations which are interacting with the mass outflows from young stars in these regions. These observations also represent the first direct detection of such high gas temperatures outside the Orion-KL region. Gas heating could be due to the radiation from the exciting sources of the compact H II regions and masers or from the input of mechanical energy due to the outflows. These warm condensations are embedded in a cooler and more extended envelope which dominates lower angular resolution studies.

Subject headings: interstellar: molecules — nebulae: H II regions — nebulae: individual

I. INTRODUCTION

Single-dish studies in the past decade of the $\lambda \approx 1.3$ cm transitions of NH_3 have demonstrated the usefulness of this molecule in determining the line opacity, temperature, density, mass, and the relative importance of collisional and radiative excitation of interstellar matter. With the completion of the Very Large Array (VLA), the highest angular resolution available for molecular line studies will be achieved with the NH_3 lines via aperture synthesis techniques. In particular, distant regions (> 10 kpc) can now be studied with a linear resolution of better than 0.1 pc.

Continuum observations in the radio and infrared of the W51 region indicate the presence of young, massive O stars, while line observations in H_2, H_2O, and SiO suggest the presence of energetic mass outflows, as have been seen in the solar neighborhood (cf. Genzel and Downes 1982). We have chosen the $(J, K) = (3,3)$ line of NH_3 in order to maximize our sensitivity to relatively dense and warm ($T_k \geq 50$–100 K) gas and to examine the detailed structure of the molecular cloud in the immediate vicinities of these distant OB stars.

II. OBSERVATIONS AND RESULTS

a) *Experimental Parameters*

Aperture synthesis maps of W51 in the $(J, K) = (3,3)$ line of NH_3 were made with the Very Large Array of the National Radio Astronomy Observatory[2] in the C configuration during 1981 November and 1982 January. A total of 18 antennas were used with a maximum baseline of 2.8 km. A K-band maser preamplifier was available during 1982 January on the innermost antenna of the east arm, improving the system temperature at $\lambda \sim 1.3$ cm by a factor of 8 (~ 100 K versus ~ 800 K) for that particular antenna. Spectral resolution was provided by 32 independent channels of 390.6 kHz (4.91 km s^{-1}) in width. The center of our spectral window was at 23870.129 MHz. The phase center of the array was at R.A. (1950) $= 19^h21^m24^s$, decl. (1950) $= 14°25'00''$.

Our primary flux calibrator was 3C 286 (we assumed 2.41 Jy at K band). We monitored every 20 minutes one of two phase calibrators, 2005+403 (R.A. [1950] $= 20^h05^m59^s.56$, decl. [1950] $= 40°21'01''.80$, $\pm 0''.05$) and 2134+004 (R.A. [1950] $= 21^h34^m05^s.205$, decl. [1950] $= 00°28'25''.08$, $\pm 0''.02$). The derived fluxes for the two calibrators were 3.8 Jy and 4.6 Jy, respectively, in 1981 November, and 3.3 Jy for 2005+403 in 1982 January. Passband calibrations were made by observing 3C 84 during 1981 November and by using the autocorrelation functions for each IF (Clark and van Gorkom 1981) during 1982 January. After independently calibrating the two sessions with the closure solutions from the

[1] Miller Fellow 1980–1982.

[2] The National Radio Astronomy Observatory is operated by Associated Universities, Inc., under contract to the National Science Foundation.

calibrators, the data bases were combined. We estimate conservatively that absolute flux densities are accurate to ~ 20% in the line maps, which are dominated by system noise. Uncertainties in phase measurements for the calibrators were $\pm 20°$. For our final maps at 3″ resolution, uncertainties in absolute positions are therefore $\pm 0\farcs3$.

The visibility data for each spectral channel were convolved with a Gaussian taper of 50 kλ (0.63 km; half-width at 30%), resulting in a beam of $2\farcs6 \times 2\farcs5$ with P.A. of 39° E of N. Fourier transformation of the visibility data produced dirty maps, which were then CLEANed with the algorithm devised by Clark (1980). The CLEAN components were then used as the input model for self-calibration (Schwab 1980). Since the continuum emission from the H II regions dominates the observed flux densities in each spectral channel, the dynamic range of our maps is improved by a factor of ~ 2 by using self-calibration.

b) *Maps*

Figure 1 (*top*) shows a continuum map of the W51 region constructed from an average of the "off-line" spectral channels covering the velocity ranges −6–28 km s^{-1} and 92–126 km s^{-1}. Single-dish observations by Matsakis *et al.* (1980) show that there is no emission at these velocities, and the outer quadrupole satellite hyperfine components for the $(J, K) = (3,3)$ line at ± 2.3 MHz (± 29 km s^{-1}) are down in intensity by a factor of ~ 30 in the optically thin limit. A subtraction of the two maps, each covering one of these velocity ranges, shows the flux densities to be equal at the 2 σ noise level of 30 mJy. The various compact and ultracompact H II regions as reported by Scott (1978) and Genzel *et al.* (1982*a*) are present in our map.

Figure 1 (*bottom*) shows the average over the velocity range 53–67 km s^{-1} after subtracting the continuum contribution (i.e., Fig. 1, *top*). We have clearly detected NH_3 emission in three small condensations associated with the most compact H II regions. At a distance of 7 kpc, the deconvolved sizes of 3″–4″ for these emission knots correspond to 0.10–0.14 pc. The NH_3 emission appears centered at ~ 60 km s^{-1}, the velocity of the densest molecular cloud associated with W51 (Mufson and Liszt 1979). In each case the NH_3 emission is displaced with respect to the H II regions. Table 1 lists the positions, fluxes, and size scales of the various objects detected.

c) *Temperatures*

Derived beam-averaged brightness temperatures T_B (BEAM) are listed in Table 1. Higher resolution maps with 100 kλ taper ($1\farcs8$ beam) show somewhat higher values: T_B(BEAM) $= 66 \pm 7$ K for the NH_3–1 cloud, and T_B(BEAM) $= 40 \pm 7$ K for the NH_3–2 and NH_3–3 clouds. This is consistent with Gaussian brightness temperature distributions and the deconvolved size scales deduced from the maps. The *peak* temperatures T_B(PEAK), corrected for the finite resolution of the beam, can then be calculated and are also listed in Table 1. Because of the irregular shape of NH_3–3, the peak value of T_B is probably higher and more consistent with the temperatures of the other two condensations.

We estimate that for NH_3–1 and NH_3–2, with a source size $\theta_s \sim 3''$ and T_B(PEAK) ~ 100 K (Table 1), T_B(BEAM) for a 40″ beam would be ~ 1 K. This is roughly 60% of the value observed by Matsakis *et al.* (1980). Considering the coarser spectral resolution of our results, we find that the warm NH_3 condensations detected with the VLA constitute the bulk of the emission detected with a 40″ beam. Some extended emission with lower surface brightness (< 40 K) is probably also present. This is suggested by observations with an even coarser angular resolution (~ 2′; Matsakis *et al.* 1980) which yielded higher antenna temperatures than expected from observations with a 40″ beam. Note that with the same arguments as above, the warm gas detected in NH_3 would contribute a minute fraction of single-dish CO spectra.

d) *Optical Depths*

With 100 kλ taper, we also detected NH_3 in *absorption* at the 5 σ level directly against W51-e2. The absorption region is immediately west of the NH_3–2 emission region and is probably part of the same cloud, which happens to lie in front of the H II region. This is consistent with the arclike appearance of NH_3–2 at 50 kλ taper (Fig. 1, *bottom*). The apparent beam-averaged optical depth is 0.17 ± 0.07. Correcting for the temperature of the absorbing gas (100–150 K), the optical depth becomes 0.3–0.5. The actual optical depth could be higher if there are structures substantially smaller than 0.1 pc so that the gas temperature exceeds T_B, or if the NH_3 cloud happens to lie in front of only part of the H II region. The latter opinion is supported by the maps since, for NH_3–1 and NH_3–2, the observed NH_3 emission lines are displaced with respect to the H II regions. In the case of W51 IRS 2 the absence of absorption at a level of 20 mJy against the peak flux of 600 mJy (at 100 kλ taper) suggests an apparent optical depth of < 0.03. Hence, if any NH_3 is in front of the H II region, it must be optically thin. If optically thick gas is behind the H II region, it must be colder than 10–20 K.

e) *Line Profiles*

We have made additional maps at 50 kλ taper covering other velocity ranges. The observed peak flux densities as a function of velocity for the three NH_3 condensations are summarized in Figure 2. The absorption feature toward W51-e2 is consistent with a flux

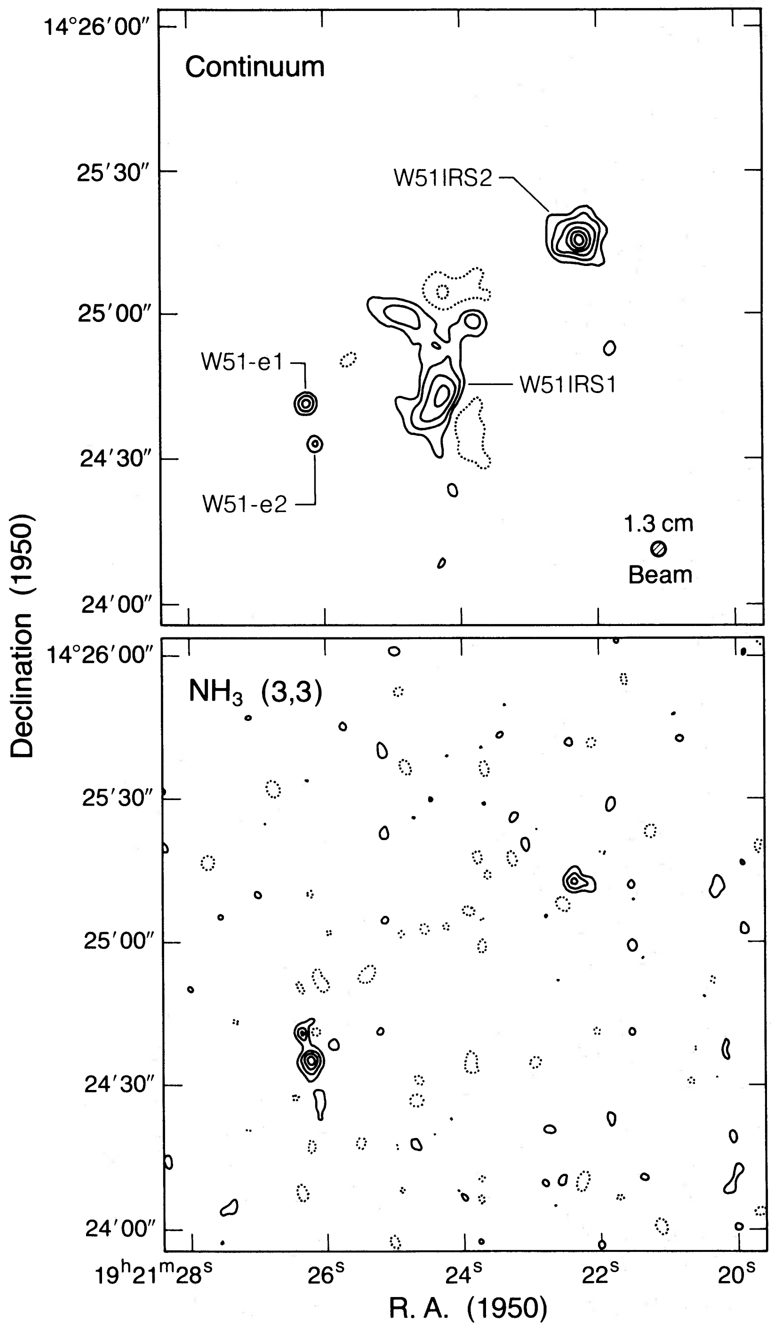

FIG. 1.—(*top*) $\lambda = 1.3$ cm continuum map of the W51 region constructed from the "off-line" channels of our spectral line observations. The velocity ranges of this map correspond to -6–28 and 92–126 km s^{-1}. The contour levels are -10%, -5%, 5%, 10%, 20%, 40%, 60%, 80%, and 100% of the peak flux density of 1.0 Jy per beam. The synthesized beamwidth is $2''.6 \times 2''.5$; the peak brightness temperature is 350 K averaged over the beam. (*bottom*) Observed $(J, K) = (3,3)$ NH_3 emission covering the velocity range 53–67 km s^{-1}, after subtraction of the continuum contribution. The contour levels are -20%, 20%, 40%, 60%, 80%, and 100% of the peak flux density of 150 mJy per beam. For the synthesized beam of $2''.6 \times 2''.5$, the peak brightness temperature is 50 K averaged over the beam.

TABLE 1

COMPACT H II REGIONS AND NH_3 CLOUDS IN W51

A. CONTINUUM

Source	R.A. (1950)	Decl. (1950)	S_ν(BEAM)[a] (Jy)	θ_{FWHM}[b] (″)	T_B(BEAM)[a] (K)	S_ν(TOTAL)[a] (Jy)
W51-e1	$19^h21^m26^s.13 \pm 0^s.01$	14°24′33″.1 ± 0″.2	0.11 ± 0.03	2.0 ± 0.1	36 ± 7	0.18 ± 0.03
W51-e2	19 21 26.26 ± 0.01	14 24 41.6 ± 0.2	0.21 ± 0.03	2.3 ± 0.1	70 ± 7	0.38 ± 0.04
W51 IRS 2 ...	19 21 22.26 ± 0.01	14 25 15.8 ± 0.2	1.05 ± 0.03	3.3 ± 0.1	350 ± 7	2.81 ± 0.10

B. LINE

Source	R.A. (1950)	Decl. (1950)	S_ν(BEAM)[a] (Jy)	θ_{FWHM}[b] (″)	T_B(BEAM)[a] (K)	T_B(PEAK)[a] (K)
NH_3-1	$19^h21^m26.25 \pm 0^s.01$	14°24′35″.1 ± 0″.2	0.15 ± 0.03	3.0 ± 0.3	49 ± 6	83 ± 14
NH_3-2[c]	19 21 26.37 ± 0.01	14 24 40.8 ± 0.2	0.09 ± 0.03	1.6 ± 0.3	30 ± 6	100 ± 30
NH_3-3	19 21 22.37 ± 0.01	14 25 12.7 ± 0.2	0.09 ± 0.03	3.9 ± 0.3	30 ± 6	42 ± 10

[a] S_ν(BEAM) and T_B(BEAM) are the peak values, averaged over the beam; S_ν(TOTAL) is the total over the map; T_B(PEAK) is the peak value assuming a Gaussian source distribution with the given θ_{FWHM}.

[b] θ_{FWHM} is the equivalent deconvolved source size. The synthesized beamwidth is 2″.6 × 2″.5.

[c] Both the source size and flux density are underestimated for this source because of absorption against the compact H II region W51-e2.

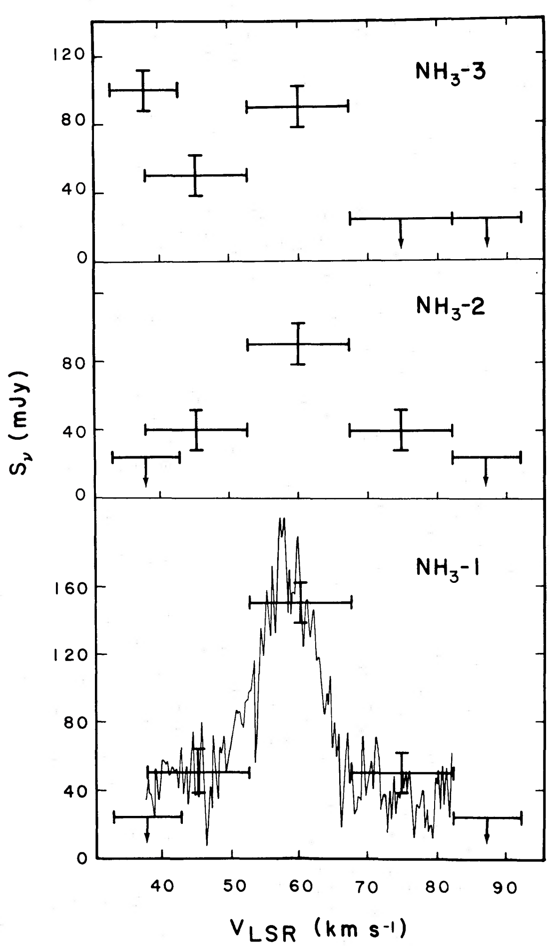

FIG. 2.—Observed spectral distributions for the three NH_3 condensations from our synthesis maps. The horizontal error bar indicates the velocity range over which we averaged for a particular map. The vertical error bar gives $\pm 1\ \sigma$ uncertainty in the flux density. Indicated fluxes are the peak flux densities per beam. Note the blueshifted emission (33–43 km s^{-1}) detected for NH_3-3. This detection is well out of the noise, and similar emission at this velocity range is not detected in the other sources. A single-dish spectrum from Matsakis *et al.* (1980) is superposed on our spectrum for NH_3-1.

density of ~ 40 mJy across the entire band, and we have omitted it in Figure 2. Superposed on the observed fluxes for NH_3-1 is a single-dish spectrum (40″ beam) toward W51 IRS 1 from Matsakis *et al.* (1980), which illustrates that the VLA spectrum is consistent with the line shape obtained with coarser angular resolution. The detection of NH_3 emission at the VLA in the velocity ranges 38–53 km s^{-1} and 67–82 km s^{-1} for NH_3-1 implies an intrinsic line width of 18 ± 8 km s^{-1} if the profile is Gaussian. Figure 2 also shows that we have detected significant emission at blueshifted velocities (33–43 km s^{-1}) toward W51 IRS 2. This detection is better than an 8 σ result because the emission is, in fact, extended (~ 5″). The emission probably does not arise from hyperfine structures (expected at ±22 and ±29 km s^{-1}) because of the absence of comparable emission at redshifted velocities. This blueshifted emission appears at the same velocities as the strong blueshifted H_2O maser emission in W51 NORTH and may be part of the same outflowing gas in IRS 2.

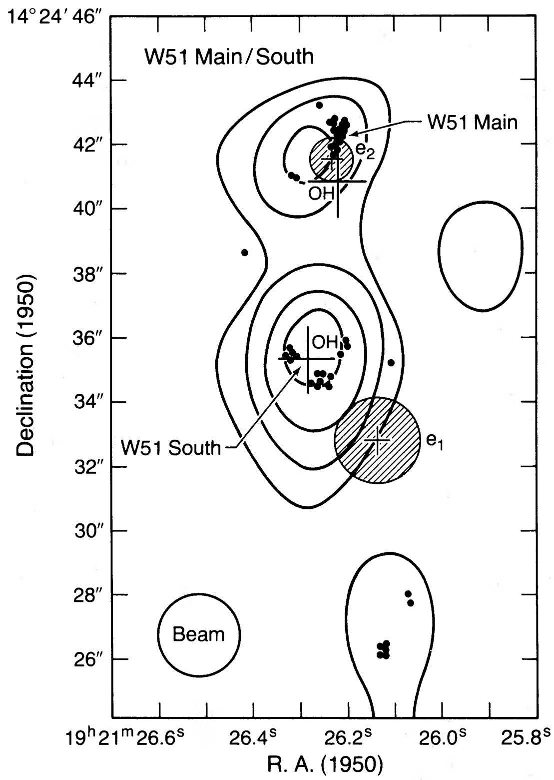

FIG. 3*a*

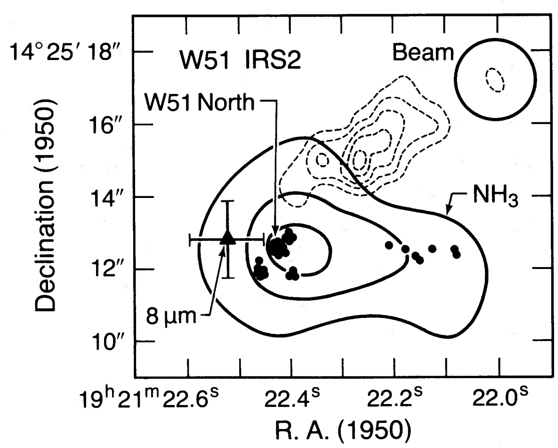

FIG. 3*b*

FIGS. 3*a*–*b*.—Schematics showing the distribution of NH_3 (*solid contours*), H_2O masers (*filled circles*), OH masers (*crosses*), and compact H II regions (*shaded circles and dashed contours*; half-power sizes). We used the higher angular resolution continuum maps from Genzel *et al.* (1982*a*) and Scott (1978). The synthesized beams are indicated. We also plot the position of an 8 μm source which probably drives the H_2O masers in W51 NORTH. Note the good correlation between the H_2O masers and the NH_3 emission.

III. DISCUSSION

a) *Interactions with the Outflows*

As mentioned earlier, observations of H_2O masers (Schneps *et al.* 1982), quadrupole lines of H_2 (Beckwith and Zuckerman 1982), and high-velocity line wings in the $v = 0, J = 2-1$ line of SiO (Downes *et al.* 1982) suggest the presence of energetic outflows in this region. In Figure 3, we show schematically the distributions of NH_3, H_2O and OH masers, and the compact H II regions. The *most* striking feature of Figure 3 is clearly the direct association of the H_2O masers with the emission peak of each of the warm NH_3 condensations. Even the cluster of weak H_2O masers 10″ southwest of W51 SOUTH lies within the first positive contour ($\sim 2\ \sigma$). The compact H II regions are displaced with respect to the NH_3 emission and are probably *not* embedded. The NH_3 condensations may therefore be adjacent density inhomogeneities as in the "blister" model (Israel 1978). Proper motion studies of the H_2O masers in W51 (Genzel *et al.* 1981; Schneps *et al.* 1981) show that the high-velocity dispersions are probably caused by mass outflow from young stars close to the maser sources. Although the observed NH_3 line widths are also significantly larger than expected for quiescent molecular cloud matter, they are smaller than the velocity dispersion of the H_2O masers. It is likely that the NH_3 gas represents turbulent material excited by and in interaction with the outflowing material.

The deduced values of T_B(PEAK) represent the first direct detection of such high gas temperatures (~ 100 K) outside the Orion-KL region. In the case of NH_3-3, there is a compact infrared source, IRS 2 EAST (Genzel *et al.* 1982*a*), within 1″ of the NH_3 peak. This infrared source, rather than the H II region W51 IRS 2, may be the source of heating and outflow. For NH_3-1 and NH_3-2 (W51 MAIN/SOUTH), compact infrared objects have not been detected. Hence, it is possible that the outflows in these cases are driven by the nearby compact H II regions e1 and e2, so that the molecular condensations are heated externally. However, it remains possible that exciting sources are embedded within the NH_3 clouds, which have escaped detection because of heavy extinction.

We note that the morphology of an NH_3 emission region displaced from a nearby source undergoing mass loss is reminiscent of the mass outflow in Cepheus A (Rodríguez, Ho, and Moran 1980; Ho, Moran, and Rodríguez 1982). An anisotropic density distribution in the vicinity of a source ejecting mass can give rise to an outflow that is anisotropic in appearance. The mostly redshifted H_2O maser emission in W51 MAIN (Genzel *et al.* 1981) and the mostly blueshifted emission in W51 NORTH (Schneps *et al.* 1981) may therefore be indicators of their positions relative to dense ambient matter. In fact, placing the H_2O masers in W51 NORTH on the far side of NH_3–3 may explain the apparently low luminosity of the H_2 lines (Beckwith and Zuckerman 1982).

b) *Comparison with the Orion-KL Region*

We find that the physical state of the dense molecular cloud matter adjacent to the compact H II regions in W51 is similar to that in the Orion-KL region. In both cases, highly excited phenomena such as high-velocity H_2O maser emission, vibrationally excited H_2, and high-velocity wings in molecular lines suggest energetic mass outflow. The present study shows that ambient cloud matter has moderately high velocity dispersions and is heated to a fairly high temperature, suggesting direct interaction with the outflows. A component of warm and dense molecular material, showing the same evidences of interaction with an outflow, has also been observed in Orion (see Plambeck *et al.* 1982; Bieging *et al.* 1982; Genzel *et al.* 1982*b*). The size scale of the warm NH_3 gas in W51 is roughly three times larger than in Orion. This may be due to the fact that the observed phenomena in W51 are more energetic as compared with Orion.

P. T. P. H. acknowledges support from NSF grant AST-78-21037 to the Radio Astronomy Laboratory. R. G. and A. D. acknowledge support from NSF grant AST-78-24453.

REFERENCES

Beckwith, S., and Zuckerman, B. 1982, *Ap. J.*, **255**, 536.
Bieging, J. H., Martin, R. N., Pauls, T., and Wilson, T. L. 1982, in preparation.
Clark, B. G. 1980, *Astr. Ap.*, **89**, 377.
Clark, B. G., and van Gorkom, J. 1981, VLA Test Memorandum No. 131.
Downes, D., Genzel, R., Hjalmarson, A., Nyman, L. A., and Ronnang, B. 1982, *Ap. J.* (*Letters*), **252**, L29.
Genzel, R., *et al.* 1981, *Ap. J.*, **247**, 1039.
Genzel, R., Becklin, E. E., Wynn-Williams, C. G., Moran, J. M., Reid, M. J., Jaffe, D. T., and Downes, D. 1982*a*, *Ap. J.*, **255**, 527.
Genzel, R., and Downes, D. 1982, in *Regions of Recent Star Formation*, ed. R. S. Roger and P. E. Dewdney (Dordrecht: Reidel).
Genzel, R., Downes, D., Ho, P. T. P., and Bieging, J. H. 1982*b*, *Ap. J.* (*Letters*), **259**, L103.
Ho, P. T. P., Moran, J. M., and Rodriguez, L. F. 1982, *Ap. J.*, **262**, 619.
Israel, F. P. 1978, *Astr. Ap.*, **70**, 769.
Matsakis, D. N., Bologna, J. M., Schwartz, P. R., Cheung, A. C., and Townes, C. H. 1980, *Ap. J.*, **241**, 655.
Mufson, S. L., and Liszt, H. S. 1979, *Ap. J.*, **232**, 451.
Plambeck, R. L., Wright, M. C. H., Welch, W. J., Bieging, J. H., Baud, B., Ho, P. T. P., and Vogel, S. N. 1982, *Ap. J.*, **259**, 617.
Rodriguez, L. F., Ho, P. T. P., and Moran, J. M. 1980, *Ap. J.* (*Letters*)., **240**, L149.
Schneps, M. H., Lane, A. P., Downes, D., Moran, J. M., Genzel, R., and Reid, M. J. 1981, *Ap. J.*, **249**, 124.
Schwab, F. 1980, *Proc. Soc. Photo-Opt. Instrum. Eng.*, **231**, 18.
Scott, P. F. 1978, *M.N.R.A.S.*, **183**, 435.

ANIRUDDHA DAS and REINHARD GENZEL: Department of Physics, University of California, Berkeley, CA 94720

PAUL T. P. HO: Department of Astronomy, Harvard University, 60 Garden Street, Cambridge, MA 02138